


Green Lead Nanoparticles Induced Apoptosis and Cytotoxicity in MDA-MB-231 Cells by Inducing Reactive Oxygen Species and Caspase 3/7 Enzymes

Dose-Response:
An International Journal
October-December 2023:1-8
© The Author(s) 2023
Article reuse guidelines:
sagepub.com/journals-permissions
DOI: 10.1177/15593258231214364
journals.sagepub.com/home/dos


Wadyan Lafi Alsulami, Daoud Ali , Bader O. Almutairi , Khadijah N. Yaseen, Saad Alkahtani , Rafa A. Almeer, and Saud Alarifi 

Abstract

Nanoparticles are widely used in the pharmaceutical, agriculture, and food processing industries. In this study, we have synthesized green lead nanoparticles (gPbNPs) by using an extract of *Ziziphus spina-christi* leaves and determined their cytotoxic and apoptotic effect on the human breast cancer MDA-MB-231 cell line. gPbNPs were characterized by using X-ray diffraction (XRD), energy dispersive X-ray (EDX) scanning electron microscope (SEM), and transmission electron microscope (TEM). The toxicity of gPbNPs was determined on the MDA-MB-231 cell line using MTT and NRU assays and as a result cell viability was reduced in a concentration-dependent manner. MDA-MB-231 cells were more sensitive at the highest concentration of gPbNPs exposure. In this experiment, we observed the production of intracellular ROS in cells, and induction of caspase 3/7 was higher in cells at 42 µg/ml of gPbNPs. Moreover, the Bax gene was upregulated and the Bcl-2 gene was downregulated and increased caspase 3/7 activity confirmed the apoptotic effect of gPbNPs in cells. Our observation showed that gPbNPs induced cell toxicity, increased generation of intracellular ROS, and gene expression of Bcl-2 and Bax in the MDA-MB-231 cell line. In conclusion, these findings demonstrated that gPbNPs executed toxic effects on the MDA-MB-231 cell line through activating caspase 3/7 activity.

Keywords

MDA-MB-231 cell line, gPbNPs, cytotoxicity, oxidative stress, apoptosis

Introduction

Nanotechnology has become one of the fastest-growing areas of science and technology and it is helping to considerably improve, and revolutionize, many technology and industry sectors such as medicine, transportation, energy, food safety, and environmental science. Nanomaterials can be used in pollution control and wastewater treatment, making water accessible to all. Not limited to the above fields, nanomaterials and nanotechnology have many applications in every field of science and engineering, leading to greater technological advancements. The products of nanotechnology have a big market, and its value was 39.2 billion dollars in 2016 and it will be 124 billion dollars in 2024.¹ Their innovative physicochemical properties enable their use in textiles, cosmetics,

and drugs, thereby increasing the possibility for human and environmental interaction with nanomaterials.² The purposeful use of nanomaterials might have happened as a result of ingesting nanomaterials containing drugs.³ Fortuitous exposure of nanomaterials to the liver occurs directly during the manufacturing and disposal of used nanomaterial products.⁴

Department of Zoology, College of Science, King Saud University, Riyadh, Saudi Arabia

Received 27 March 2023; accepted 30 October 2023

Corresponding Author:

Saud Alarifi, Department of Zoology, College of Science, King Saud University, Riyadh 11451, Saudi Arabia.
Email: salarifi@ksu.edu.sa



Creative Commons Non Commercial CC BY-NC: This article is distributed under the terms of the Creative Commons Attribution-NonCommercial 4.0 License (<https://creativecommons.org/licenses/by-nc/4.0/>) which permits non-commercial use, reproduction and distribution of the work without further permission provided the original work is attributed as specified on the SAGE and Open Access pages (<https://us.sagepub.com/en-us/nam/open-access-at-sage>).

Workers involved in the development, production, and use of new nanoparticles are already exposed to uncertain levels of toxicity.⁵ Silver nanoparticles are frequently used in skin care products.⁶ Occupational exposure to NPs could be associated with an increased risk of various cancers. The underlying mechanisms of nanomaterial toxicity are not yet cleared, but there is little evidence that reactive oxygen species (ROS) play important roles in the toxicity and carcinogenetic effects of metals.⁷

Thus, nanomaterials produced cytotoxicity in cells due to the accumulation of metal ions.⁸ The human breast is an important organ of the human body and has a major role in child feeding. So in this study we used green lead nanoparticles (gPbNPs) to find out their anticancer activity on human breast cancer MDA-MB-231 cell lines. Some reports detected variation in cytotoxicity among normal cells transformed cells and cell lines for NPs. Iron oxide NPs induced reacted toxicity in the lung cancer cell lines instantly and did not in IMR-90 fibroblast line.⁸ NP-mediated toxicity involves various mechanisms, in particular the production of excess reactive oxygen species (ROS). As is well known, mitochondrial dysfunction is the major source of ROS overload.⁹ Oxidative stress has mainly resulted from the generation of reactive oxygen species (ROS). Excessive ROS causes the imbalance of oxidation and antioxidant system in the body, which may induce lipid peroxidation and change various enzymatic activities.¹⁰ Oxidative stress and apoptotic response are key molecular mechanisms to induce the toxic effects of xenobiotics.¹¹ To my knowledge, there are no studies that confirmed the adverse effects of gPbNPs on human breast cancer MDA-MB-231 cell lines.

Materials and Methods

Chemical and Reagents

MTT (3-(4, 5-dimethylthiazol-2-yl)-2, 5-diphenyltetrazolium bromide), 2, 7-dichlorofluorescein diacetate (H2-DCFH-DA), neutral red uptake dye, Annexin V-FITC, and propidium iodide were purchased from Sigma-Aldrich (St. Louis, Missouri, United States). Dulbecco's modified Eagle's medium (DMEM), fetal bovine serum (FBS), and antibiotics were purchased from Gibco, USA. Lead acetate was purchased from Merck & Co., Inc. NY USA.

Green Synthesis of Lead Nanoparticle From *Ziziphus spina-christi* Leaf Extract

Ziziphus spina-christi leaf was collected from the local area of Riyadh, Saudi Arabia, and washed and oven-dried at 50°C until the dry weight is stabilized. The plant was recognized by Dr Thomas, taxonomist, Department of Botany at King Saud University, Riyadh, Saudi Arabia. The dried leaves were blended in powder. 50 gm powder was mixed in 100 mL of Milli-Q deionized water in a 250 ml glass conical flask and

stored at 4°C for 72 h and boiled for 30 min. The aqueous extract was separated by filtration with Whatman filter paper and then centrifuged at 1,3000 rpm for 5 min to remove heavy biomaterials. Aqueous extract of *Ziziphus spina-christi* leaf (25 mL) was mixed with 50 mL of (0.5 M) lead acetate solution to prepare Pb nanoparticle via the precipitation reaction method. 25 mL extract of *Ziziphus spina-christi* leaf was mixed with 5 mL of lead acetate solution (0.5 M) in a 100 mL conical flask. After mixing Pb (II) acetate solution, color was changed to light greenish white due to the reduction of Pb (II), and ascorbic acid (.1 M) solutions were mixed drop by drop into the conical flask to stabilize the reaction.

After the reaction was ended, the suspension was mixed at 500 rpm for 24 hours at 30°C. Finally, the precipitate was filtered and rinsed with a solution before being washed with distilled water 3 times. The precipitated materials were dried in the oven at 150°C for 4 hours. The Pb nanoparticle was collected and stored at room temperature. The dried powder was ground.

Characterization of Nanomaterials

gPbNPs were characterized using energy-dispersive X-ray spectroscopy (JEM-2100F) (JEOL, Japan), scanning electron microscope (SEM), and transmission electron microscope (TEM) (JEOL Inc., Tokyo, Japan) operated at 110 kV.

Cells and Exposure of gPbNPs

MDA-MB-231 cell line was procured from American Type Culture Collection (ATCC), USA. These cells were sub-cultured in DMEM with 10% FBS and 10,000 U/ml antibiotics in a 5% CO₂ incubator at 37°C. The cells at 80% confluence were sub-cultured into 96 well plates, 6 well plates, and 25 cm² flasks according to designed experiments.

The stock solution of gPbNPs was made in double distilled water at the rate of 10 mg NPs/10 mL deionized water and diluted according to the experimental concentration (0–120 µg/ml). Control cells were not treated with NPs and were considered as controls in each experiment.

MTT Test. The mitochondrial activity was determined by the MTT test.¹² The cells were seeded in 96-well plates and exposed to various gPbNPs concentrations for 24 hour. After being exposed to gPbNPs for 24 hour, the suspension was removed from the plate and the cells were washed in PBS. MTT solution (100 µl) was mixed in each well at a final concentration of .5 mg/mL and incubated for an additional 3.5 hour. The formed formazan crystal was dissolved in isopropanol, and the absorbance was measured at 570 nm using a BioTek Epoch plate reader (BioTek Instruments, Winooski, VT, USA) and Gen5 software (version 1.09).

The half-maximal inhibitory concentration (IC₅₀) 24 hour of gPbNPs was determined on the MDA-MB-231 cell line by using the MTT test result. Based on IC₅₀ 24 hour of gPbNPs,

we have determined 3 sub-lethal concentrations in further experiments in this study as shown in [Table 1](#).

Neutral Red Uptake (NRU) Assay. A neutral red uptake assay was used to evaluate the viability of cells according to Reference 13. The cells were seeded in 96-well plates and exposed to various gPbNPs concentrations for 24 hour. After being exposed to gPbNPs for 24 hour, the suspension was removed from the plate and the cells were washed in PBS. Then, the plate was mixed with neutral red staining (.5 mg in 10 mL complete media), and the plate was incubated for 4 hour. After 4 hour, the cells were fixed using a fixative solution (.5 gm calcium chloride [CaCl₂] and 2.5 mL formaldehyde) and the dye was removed using a solution of acetic acid, absolute ethanol, and water. After 15 minutes, the plate was shaken for 15 minutes at room temperature, and the plate was measured at 540 nm using a BioTek Epoch plate reader (BioTek Instruments, Winooski, VT, USA) and Gen5 software (version 1.09).

Intracellular Reactive Oxygen Species (ROS) Generation

Generation of intracellular ROS in the MDA-MB-231 cell line after exposure to gPbNPs (0, 14, 28, and 42 µg/ml) for 24 hour was measured according to the method in Reference 14. Cells (3×10^4) were cultured in a black bottom culture plate (96 well) and incubated at 37°C in a CO₂ incubator for 24 hour for attachment. After exposure, the culture plates were washed with chilled PBS and 10 µM DCFH-DA was added per well and the culture plate was incubated at 37°C in a CO₂ incubator for 30 minutes. After incubation, the plate was washed and fluorescence intensity was measured at 485 nm excitation and 535 nm emissions using the microplate reader (Synergy-H1; BioTek). Data were represented as a per cent of fluorescence intensity relative to the control wells. The cells (3×10^4 cells/well) were seeded in a 6-well transparent plate and exposed to different concentrations of gPbNPs for 24 hour. After exposure, cells were washed with PBS and 10 µM DCFH-DA was added per well and the culture plate was incubated at 37°C in a CO₂ incubator for 30 minutes. The cell images were captured at 485 nm using a fluorescence microscope (Olympus CKX 41; Olympus: Center Valley, Pennsylvania, USA), with 40× magnification.

Measurement of Caspase 3/7 Activity

After exposure to different concentrations of gPbNPs for 24 hour, the cells were washed with PBS scraped with a scraper in lysis solution and split by using a sonicator. After that, the cell samples were used for the detection of caspase 3/7 activity as per the kit's instructions (Item No. 10009135,

Table 1. Half-Maximal Inhibitory Concentration (IC₅₀) and Standardized Dose Concentrations for gPbNPs Were Experimented on the MDA-MB-231 Cell Line.

IC ₅₀ 24 h = 55.86 µg/mL of gPbNPs	
Percentage %	Concentrations
25% IC ₅₀	14 µg/mL
50% IC ₅₀	28 µg/mL
75% IC ₅₀	42 µg/mL

Cayman Chemical 1180 East Ellsworth Road Ann Arbor, Michigan 48108 USA).

Expression of Apoptotic Genes via the Quantitative Reverse Transcriptase Polymerase Chain

Ribonucleic Acid (RNA) Isolation. The MDA-MB-231 cell line was cultured in 75 cm² flasks and incubated for 24 hour at 37°C in a CO₂ incubator. The MDA-MB-231 cell line was treated with gPbNPs (14, 28, and 42 µg/mL, respectively) for 24 hour. After exposure to cells, RNA was extracted from the cell line by using 1 mL of guanidinium thiocyanate (TRIzol) reagent and precipitated by sodium acetate. Then, TRIzol/cell lysate was transferred into the Eppendorf tube and vortexed. After 5 minutes of incubation, 200 µl of chloroform was added. Cells were incubated at room temperature for 2 minutes and centrifuged at 4200 rpm for 15 minutes at 4°C. After centrifugation, three layers were observed. Carefully transferred the 400 µl of the upper aqueous phase, which contains the RNA, into a new tube.

Then, the aqueous phase was mixed with 500 µl of isopropanol. The mixture was centrifuged for 20 minutes at 14,000 rpm. After discarding the isopropanol, 1 mL of 75% ethanol in diethyl pyrocarbonate (DEPC) was added, and it was gently mixed. Then, the previous step was carried out twice after centrifugation at 3500 rpm for 5 minutes. After that, the pellet was dissolved in 22 µl of DEPC water after the supernatant had been removed gently. The purity and concentration of the RNA were determined by using a nano-drop spectrophotometer (ND-1000; Thermo Scientific, South San Francisco, CA, USA) and stored at -80°C.

cDNA Synthesis and qRT-PCR. The cDNA of each RNA extract (1 µg) was synthesized using PCR and gene-specific DNA fragments were amplified. Then, agarose gel electrophoresis was used to visualize DNA bands. The assay was performed according to the manufacturer's protocol. RT-PCR (Thermo Scientific™, USA) was used for the detection and quantification, and glyceraldehyde-3-phosphate dehydrogenase (GAPDH) was used as the reference gene. The primer sequences of Bax and Bcl-2 genes (Macrogen, Inc., Seoul, Korea) are shown in [Table 2](#).

Statistical Analysis

Data were analyzed by using SPSS 26.0 software (IBM) and expressed as mean \pm standard error (SE). Statistical differences between the control group and exposed groups were determined by a one-way ANOVA test with the least-significant difference test. The values of $*P \leq .05$ and $**P \leq .0001$ vs control were considered statistically significant and highly significant, respectively.

Results

Properties of gPbNPs

The nature of gPbNPs as nanoparticles was examined by using EDX, SEM, and TEM. Figure 1A–C showed the EDX spectra, particles shape by SEM, and size of particles by TEM. The shape of gPbNPs was polygonal (Figure 1B). The average size of NPs was 33.8 ± 1.95 nm (Figure 1C). After the suspension of gPbNPs in Mille Q water, their size was determined using zeta sizer, and size and zeta potential were 200 ± 3.0 nm and ~ 12.4 mV, respectively.

Cell Viability

MTT assay was used to evaluate the cytotoxic activity of gPbNPs by measuring the conversion of tetrazolium dehydrogenase to water-insoluble formazan crystals, and this reduction reaction occurs in the mitochondria of living cells. The MTT results demonstrated that the viability of MDA-MB-231 cells was decreased with gPbNPs interaction and in a dose-dependent manner (Figure 2A). In MDA-MB-231 cells, the cell viability according to MTT assay was observed for gPbNPs at 24 hour as 78, 77, 75, 67, 64, 57, and 43%, as shown in Figure 1A, for concentrations of 2, 4, 8, 16, 32, 64, and 100 $\mu\text{g/mL}$, respectively, and the cell viability was highly significantly decreased ($P < .0001$) when cells were treated with gPbNPs as compared with the control.

Interpretation of MTT assay results determined the half-maximal inhibitory concentration (IC_{50})-24 hour of gPbNPs for MDA-MB-231 cells was calculated as the concentration required to inhibit the growth of cancer cells in culture by 50% compared to the untreated cells. The gPbNPs at 55.86 $\mu\text{g/mL}$ decreased the viability of MDA-MB-231 cells to 50%, and this was selected as the IC_{50} -24 hour of gPbNPs for MDA-MB-231 cells (Table 1).

The integrity of lysosomes in MDA-MB-231 cells exposed to gPbNPs was assessed by an NRU assay. This assay provides a quantitative estimation of the number of viable cells to incorporate and bind the supravital dye neutral red in the lysosomes. The cytotoxic effects were also confirmed in control samples and samples treated with gPbNPs via the NRU assay. The NRU assay result is very similar to the MTT assay result for MDA-MB-231 cells and shows a similar trend (Figure 1B). Like the MTT assay, the NRU assay shows that at

Table 2. Primer Sequences of GAPDH, Bax, and Bcl-2 Genes.

Primer		Sequence
GAPDH	Forward	5'-CTTTTGCCTCGCCAGGTGAA-3'
	Reverse	5'-GAAAACGCAGCGGTCCACTT-3'
Bax	Forward	5'-ATGTTTICTGACGGCAACTTC-3'
	Reverse	5'-AGTCCAATGTCCAGCCCAT-3'
Bcl-2	Forward	5'-ATGTGTGTGGAGACCGTCAA-3'
	Reverse	5'-GCCGTACAGTTCCACAAAGG-3'

the initial concentration of gPbNPs, the viability of cancer cells was not significantly affected, but when the concentrations of gPbNPs rise, cell growth reduced. After exposure of gPbNPs to MDA-MB-23 cells, the cell viability by NRU assay at 24 hour was 84, 83, 78, 74, 67, 56, and 55%, respectively, as shown in Figure 1B, for concentrations of 2, 4, 8, 16, 32, 64, and 100 $\mu\text{g/mL}$.

Oxidative Stress

The ability of gPbNPs to induce oxidative stress was evaluated by measuring reactive oxygen species. The treatment of cells with gPbNPs resulted in the induction of ROS production (Figure 3). As shown in Figure 3A–B, there was an increase in the level of ROS in a concentration-dependent manner. The maximum level of ROS generation was induced by the highest used concentration of 42 $\mu\text{g/mL}$, while the minimum level of ROS production was closely correlated with the lowest concentration of 14 $\mu\text{g/mL}$ compared to the control group (Figure 3A–B). The results confirmed that ROS-induced gPbNPs were a critical factor for human breast cancer cells (MDA-MB-231) that plays an important role in the induction of apoptosis. The treated MDA-MB-231 cells were examined by using a fluorescence microscope to confirm ROS activity. The images showed that the ROS production was exceeded after treatment with different concentrations (14, 28, and 42 $\mu\text{g/mL}$ of IC_{50} values-24 hour) of gPbNPs stained with DCFDA fluorescence dye (Figure 3B). The intensity of the fluorescence dye was increased in a dose-dependent manner, as shown in Figure 3B. MDA-MB-231 cells showed a higher density of dichlorofluorescein as a marker of intracellular ROS generation at the highest used concentration of 42 $\mu\text{g/mL}$, than the control (Figure 3B).

Apoptosis

We have determined the activity of caspase 3/7 in MDA-MB-231 cells. Activities of caspase 3/7 were increased according to dose-dependent and its level was increased in MDA-MB-231 cells as the dose of treatment increased (Figure 4). The apoptosis process is regulated by several key genes encoding proteins that trigger cell death. The results of Bax and Bcl-2 gene expression are shown in Figure 5. All data were

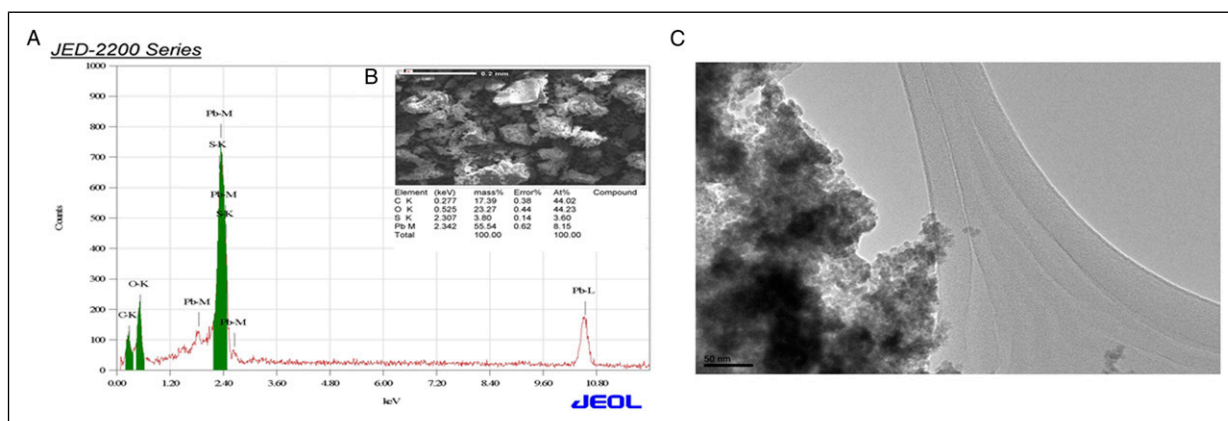


Figure 1. Characterization of gPbNPs: (A) EDX spectrum, (B) image of gPbNPs by scanning electron microscope, and (C) image of gPbNPs by transmission electron microscope (JEM 1011).

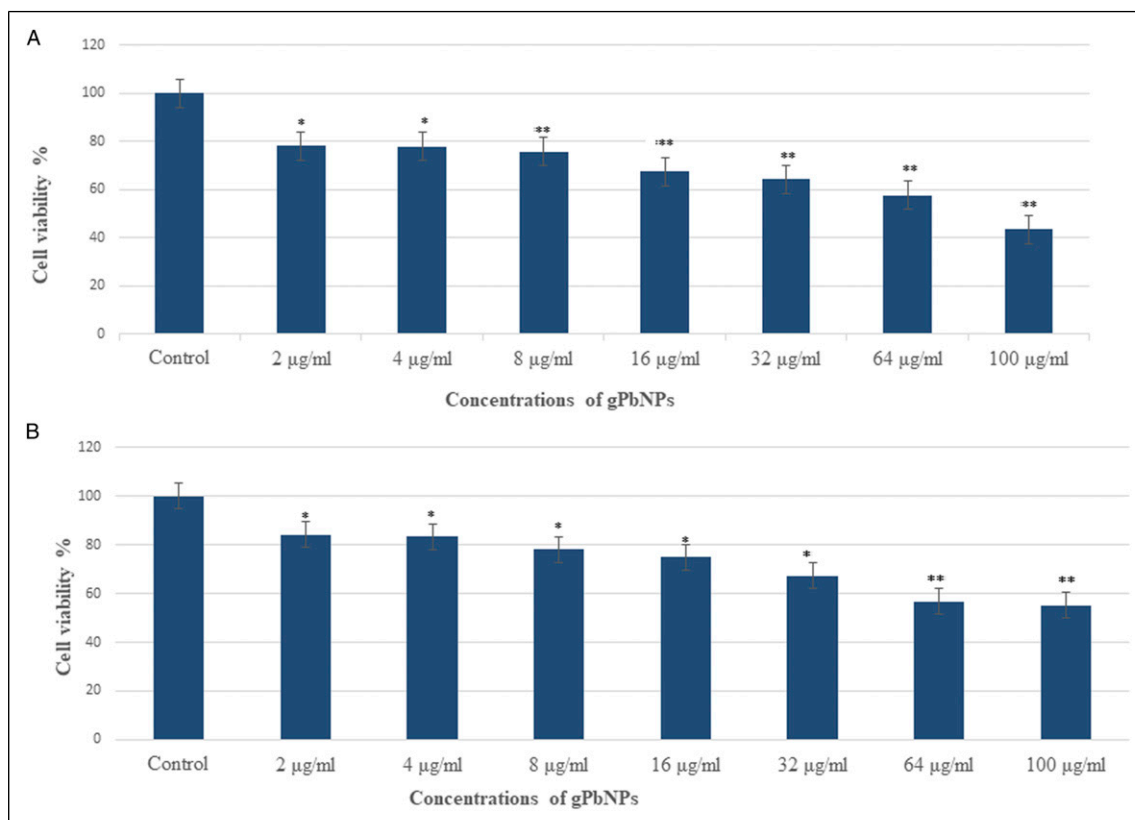


Figure 2. Cytotoxicity assessment in the MDA-MB-231 cell line after exposure to different concentrations of gPbNPs for 24 hour: (A) MTI assay and (B) NRU assay. * $P < .05$ and ** $P < .01$ vs control.

normalized with GAPDH reference gene expression level. According to the results, a significant increase in Bax ($P \leq .05$) and a significant decrease in Bcl-2 ($P \leq .05$) gene expression were observed in the groups treated with 14, 28, and 42 µg/mL compared to the control group. The gPbNPs induced apoptosis by upregulation of Bax and downregulation of Bcl-2, in a dose-dependent manner (Figure 5).

Discussion

Currently, nanotechnology is a broad field of science that is more beneficial to human life than ever before. In this experiment, we synthesized green lead nanoparticles by using an extract of *Ziziphus spina-christi* leaf and lead acetate. Plant extract-based synthetic procedures have drawn consideration

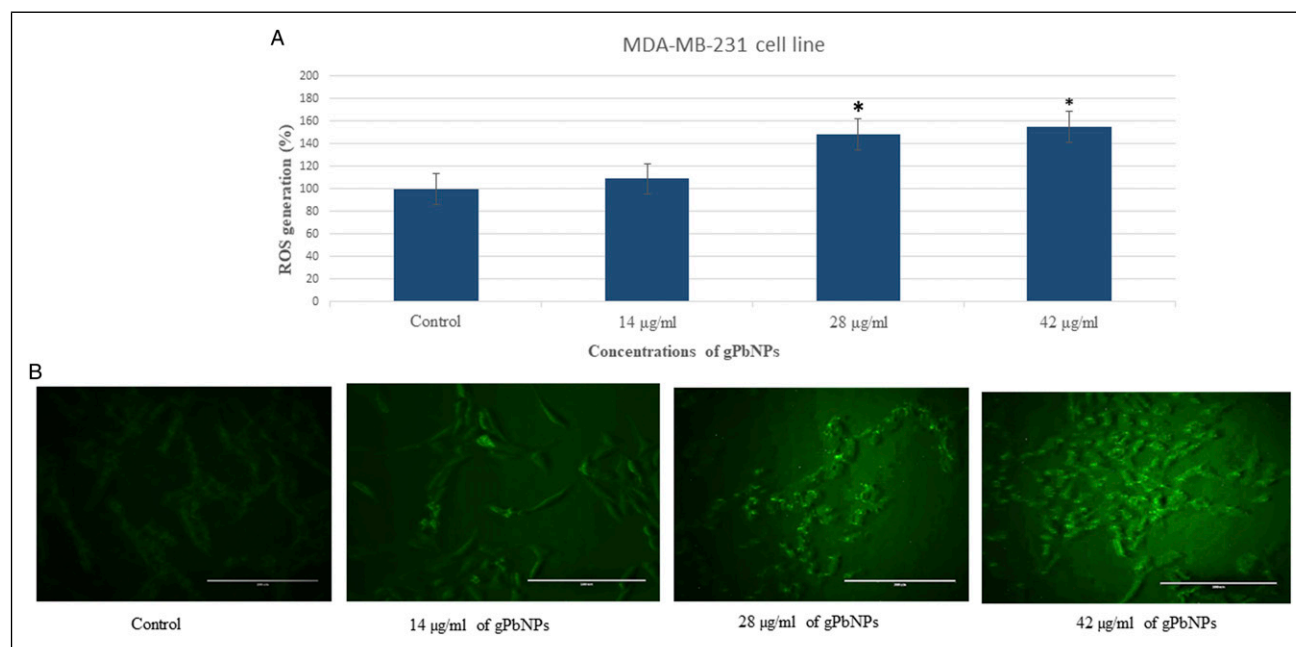


Figure 3. (A) Percentage change in intracellular ROS generation in the MDA-MB-231 cell line. (B) Generation of green fluorescence in the MDA-MB-231 cell line after exposure to various concentrations of gPbNPs for 24 hour. * $P < .05$ vs control. Scale bar is 50 µm.

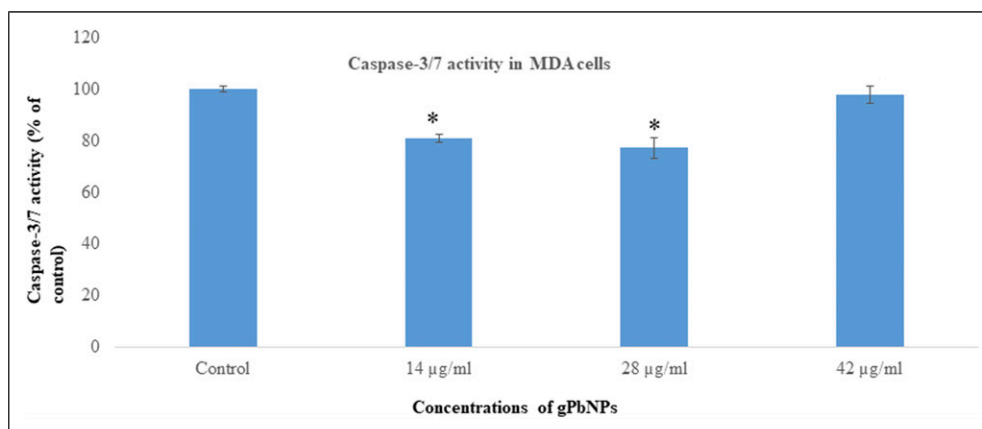


Figure 4. Caspase 3/7 activity in MDA-MB-231 cell line after exposure to gPbNPs. Each value represents the mean \pm SE of three experiments. * $P < .05$ vs control.

over conventional methods like physical and chemical procedures to synthesize nanomaterials. Greener synthesis of nanomaterials has become an area of interest because of numerous advantages such as non-hazardous, economical, and feasible methods with a variety of applications in biomedicine, nanotechnology and nano-optoelectronics, etc.

Before exposure of gPbNPs to cells, we characterized the nature and size of nanoparticles using EDX, SEM, TEM, and zeta-sizers. TEM analysis showed that the average size of synthesized NPs was 33.8 \pm 1.95 nm with polygonal and rectangular structures (Figure 1). References 15,16 reported that the size of synthesized nanoparticles depends upon plant

extract volume. Nanoparticles are more biocompatible than conservative therapeutic agents, and the substantial study aims to enhance the bioavailability of NPs for therapeutic applications in diseases such as cancer. Reference 17 evaluated the cytotoxicity and apoptotic effects of gPbNPs using MDA-MB-231 cells to determine their toxicity. The MTT assay measured metabolic activity, and the results indicate a decrease in cell viability with increasing concentrations of gPbNPs suggesting that a greater number of gPbNPs could accumulate within cells leading to increased stress and ultimately cell death. These results demonstrated the enhanced efficacy of gPbNPs against breast cancer cells. They inhibited

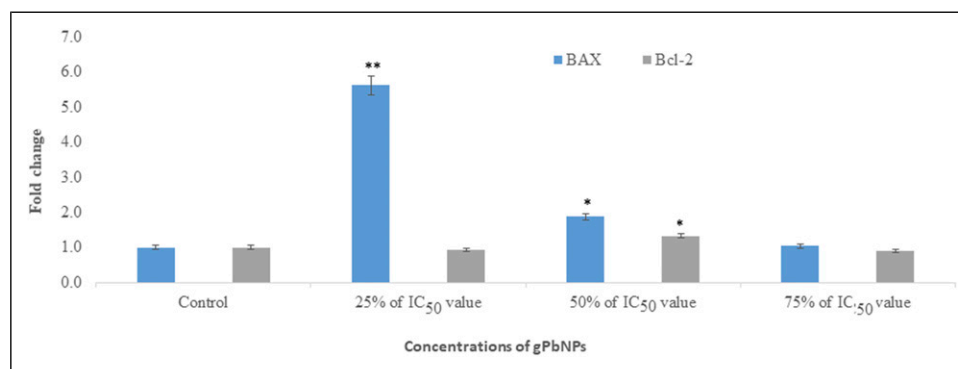


Figure 5. RT-PCR assessed and upregulated the expression of Bax and Bcl-2 gene in the MDA-MB-231 cell line after exposure to different concentrations of gPbNPs for 24 hour. * $P < .05$ and ** $P < .01$ vs control.

the MDA-MB-231 cells with an IC_{50} value-24 hour of 55.86 $\mu\text{g/mL}$, respectively.

Furthermore, the results of the MTT assay were correlated with the results of the NRU assay. The NRU assay measured the integrity of lysosomes because it reflects the ability of viable cells to incorporate the vital dye into these organelles, and the results indicate that the uptake of MDA-MB-231 cells was in a dose-dependent manner, reducing their cell viability at all concentrations. However, the NRU assay showed slightly lower cytotoxicity than the MTT assay. In contrast, these findings were consistent with Reference 18 which reported that the MTT assay indicated high anticancer activity for both Zi-AuNPs and *Ziziphus spina-christi* extract against human breast cancer cells with IC_{50} values of 48 g/mL and 40.25 g/mL , respectively.

The majority of cytotoxic agents can induce apoptosis. The excessive production of ROS in mitochondria may contribute to this pathological condition. The ROS production may result in mitochondrial permeability disruption and the release of apoptosis-triggering proteins. Therefore, anti-cancer agents that induce ROS can play a significant role in therapeutic strategy by arbitrating apoptotic pathways. Remarkably, the results showed that gPbNPs increased ROS levels in MDA-MB231 cells in a dose-dependent manner, suggesting that gPbNPs induced apoptosis in MDA-MB231 cells. Reference 19 reported that Cu-ZnNPs induced intracellular ROS generation through mitochondrial pathways in MCF-7 cells, revealing their cytotoxic activity. The pathway involved in apoptotic cell death is crucial in developing potential anti-cancer agents.²⁰ The RT-PCR was used to investigate the balance between upregulation of the pro-apoptotic gene (Bax) and downregulation of the anti-apoptotic gene (Bcl-2) in a dose-dependent manner, indicating significant induction of apoptosis in cells treated with gPbNPs in MDA-MB-231 cells. These data may be in part attributed to the increased efficacy of apoptosis in MDA-MB231 cells induced by gPbNPs. As a supportive model, Reference 21 reported that *Ziziphus spina-christi* leaf extracts also significantly increased the expression level of Bax and Bcl-2 genes in MCF-7 cells. In another study,

Reference 22 confirmed that the aqueous extract of *Ziziphus jujube* on MCF-7 showed increased expression levels of Bax, except for Bcl-2, which was inversely proportional to the time and concentration of the extract. Activation of caspase-3 was accompanied by the downregulation of Bcl-2 and the upregulation of Bax genes. All these events indicated the signs of apoptosis, which were observed more in MDA-MB231 cells after exposure to NPs. In future, we will do investigations about the mechanism of toxicity due to gPbNPs in in vivo experiments.²³

Declaration of conflicting interests

The author(s) declared no potential conflicts of interest with respect to the research, authorship, and/or publication of this article.

Funding

The author(s) disclosed receipt of the following financial support for the research, authorship, and/or publication of this article: This research was funded by Researchers Supporting Project number (RSP2023R27), King Saud University, Riyadh, Saudi Arabia.

ORCID iDs

Daoud Ali  <https://orcid.org/0000-0002-1045-4984>

Bader O. Almutairi  <https://orcid.org/0000-0002-4697-5204>

Saad Alkahtani  <https://orcid.org/0000-0001-7381-5110>

Saud Alarifi  <https://orcid.org/0000-0001-9824-5089>

References

1. Research and Markets. *Global Nanotechnology Market 2018-2024: Market Is Expected to Exceed US\$ 125 Billion*. 2018. Available at: <http://www.researchandmarkets.com>.
2. Nel A, Xia T, Mädler L, Li N. Toxic potential of materials at the nanolevel. *Science*. 2006;311:622-627. doi:10.1126/science.1114397.
3. De Jong WH, Borm PJA. Drug delivery and nanoparticles: Applications and hazards. *Int J Nanomed*. 2008;3(2):133-149.

4. Gupta R, Xie H. Nanoparticles in daily life: Applications, toxicity and regulations. *J Environ Pathol Toxicol Oncol*. 2018; 37(3):209-230.
5. Rim KT, Song SW, Kim HY. Oxidative DNA damage from nanoparticle exposure and its application to workers' health: A literature review. *Saf Health Work*. 2013;4:177-186.
6. Miethling-Graff R, Rumpker R, Richter M, et al. Exposure to silver nanoparticles induces size- and dose-dependent oxidative stress and cytotoxicity in human colon carcinoma cells. *Toxicol Vitro*. 2014;28:1280-1289.
7. Waris G, Ahsan H. Reactive oxygen species: Role in the development of cancer and various chronic conditions. *J Carcinog*. 2006;5:14.
8. Fröhlich E. Cellular targets and mechanisms in the cytotoxic action of non-biodegradable engineered nanoparticles. *Curr Drug Metabol*. 2013;14(9):976-988.
9. Schumacker PT, Gillespie MN, Nakahira K et al. Mitochondria in lung biology and pathology: More than just a powerhouse. *Am J Physiol Lung Cell Mol Physiol*. 2014;306(11):L962-L974.
10. Zhuang C, Wang Y, Zhang Y, Xu N. Oxidative stress in osteoarthritis and antioxidant effect of polysaccharide from angelica sinensis. *Int J Biol Macromol*. 2018;115:281-286.
11. El-Sayed IH, Huang X, El-Sayed MA. Surface plasmon resonance scattering and absorption of anti-EGFR antibody conjugated gold nanoparticles in cancer diagnostics: applications in oral cancer. *Nano Lett*. 2005;5:829-834.
12. Alarifi S, Ali D, Alkahtani S. Nanoalumina induces apoptosis by impairing antioxidant enzyme systems in human hepatocarcinoma cells. *Int J Nanomed*. 2015;10(1):3751-3760.
13. Alarifi S, Ali D, Alkahtani S. Oxidative stress-induced DNA damage by manganese dioxide nanoparticles in human neuronal cells. *BioMed Res Int*. 2017;2017:5478790.
14. Ali D. Oxidative stress-mediated apoptosis and genotoxicity induced by silver nanoparticles in freshwater snail *Lymnea luteola* L. *Biol Trace Elem Res*. 2014;162(1-3):333-341.
15. Moosa AA, Ridha AM, Al-Kaser M. Process parameters for green synthesis of silver nanoparticles using leaves extract of aloe vera. *Plant International J Multidis Cur Res*. 2015;3: 966-975.
16. Ahmed S, Ahmad M, Swami BL, Ikram S. A review on plants extract mediated synthesis of silver nanoparticles for antimicrobial applications: A green expertise. *J Adv Res*. 2016;7(1):17-28.
17. Joshi S, Hussain MT, Roces CB, et al. Microfluidics based manufacture of liposomes simultaneously entrapping hydrophilic and lipophilic drugs. *Int J Pharm*. 2016;514:160-168.
18. Hosny M, Eltaweil A, Mostafa M, et al. Facile synthesis of gold nanoparticles for anticancer, antioxidant applications, and photocatalytic degradation of toxic organic pollutants. *ACS Omega*. 2022;7:3121-3133.
19. Liu C-W, Lee T-L, Chen Y-C, et al. PM2.5-induced oxidative stress increases intercellular adhesion molecule-1 expression in lung epithelial cells through the IL-6/AKT/STAT3/NF- κ B-dependent pathway. *Part Fibre Toxicol*. 2018;15:4.
20. Jabir M, Saleh M, Sulaiman M, et al. (2021) Green synthesis of silver nanoparticles using annona muricata extract as an inducer of apoptosis in cancer cells and inhibitor for NLRP3 inflammasome via enhanced autophagy. *Nanomaterials*. 11(2):384.
21. Ghaffari K, Ahmadi R, Saberi B, Moulavi P. Anti-proliferative effects of *Ziziphus spina-christi* and *Phlomis russeliana* leaf extracts on HEK293 and MCF-7 cell lines and evaluation of Bax and Bcl-2 genes expression level in MCF-7 cells. *Asian Pac J Cancer Prev APJCP*. 2021;22(2):81-87.
22. Pillai RG. Antiproliferative actions of *Ziziphus jujube* fruit extract is mediated through alterations in Bcl2-Bax ratio and through the activation of caspases. *Chemical Biology Letters*. 2020;7(1):41-46.
23. Bradford MM. A rapid and sensitive method for the quantitation of microgram quantities of protein utilizing the principle of protein dye binding. *Anal Biochem*. 1976;72:248-254.